

A SUPERVISED CLASSIFICATION OF MULTI-CHANNEL HIGH-RESOLUTION SAR DATA

Dirk Borghys¹ and Christiaan Perneel²

1. Royal Military Academy, Signal & Image Center, Brussels, Belgium;
[Dirk.Borghys\(at\)rma.ac.be](mailto:Dirk.Borghys(at)rma.ac.be)
2. Royal Military Academy, Dept. of Applied Mathematics, Brussels, Belgium

ABSTRACT

Many methods have been proposed in literature for the supervised classification of multi-channel (polarimetric and/or multi-frequency) SAR data. Most of them are based on the extraction of a set of features from the original SAR data. In this paper the influence of these features on the results of the classification is examined in a quantitative manner. A set of multi-channel (P, L, C and X band) SAR data was acquired by an airborne system over a site in Southern Europe. A ground-truth mission defined the classes for learning and validation. A feature-based classification method, based on logistic regression, is used for detecting each of the classes. Logistic regression combines the input features into a non-linear function, the logistic function, in order to distinguish that class from all others. For each class a 'detection image', with a well-defined statistical meaning, is obtained. The value at each pixel in the detection image represents the conditional probability that the pixel belongs to that class, given all input features. The logistic regression is performed using a step-wise method in which, at each step, the most discriminating feature is added to the selected feature set, but only if its addition contributes significantly to the detection. The logistic regression thus also performs a feature selection. Moreover, logistic regression allows combining input data with very diverse statistical distributions.

The main aim of the current paper is to investigate the usefulness of each feature for the detection of the different classes.

Keywords: Polarimetric multi-channel SAR, supervised classification of SAR data.

INTRODUCTION

This article presents a method for supervised feature-based classification of multi-channel SAR data and examines the influence of the different features on the classification performance. The presented classification method was applied in a project on humanitarian demining. It was delivered as one of the tools that aim at helping a human operator to decide whether a region is potentially mined or not. The experts of a Mine Action Centre defined relevant land-cover classes. A set of multi-channel SAR data, including polarimetric and dual-pass interferometric data at different frequencies was acquired using the E-SAR system of the German Aerospace Centre (DLR). The images from different bands (P, L, C and X-band) cover the same region but each band has a different spatial resolution. Geocoding information was also provided.

A ground survey mission collected the necessary ground truth information for each of the defined classes.

For the classification of polarimetric SAR (POLARSAR) images, several unsupervised approaches have been proposed, based on various polarimetric decomposition methods (1). The most used method is the decomposition of Cloude and Pottier (2). In this method the polarimetric information is converted into three parameters (entropy H , angle α and anisotropy A) to which the authors have associated an elegant physical interpretation. They sub-divided the feature space formed by the three parameters into regions that correspond to distinct scattering behaviours. However, the

exact borders of these different regions depend on many factors. Different methods were suggested to make these borders flexible.

In (3) the samples in the feature space, spanned by the three Cloude parameters, are regrouped based on the complex Wishart distribution. In (4) a supervised classification method based on neural networks and fuzzy logic is used to learn the class borders from the available learning samples. The advantage of the approach is that other input features can be easily added in order to increase the discrimination ability of the classification. In (4) the largest eigenvalue (λ_1) of the polarimetric coherence matrix and the interferometric coherence ρ are added to the feature set.

In (5) a supervised classification is proposed based on the complex Wishart distribution of the polarimetric covariance matrix. This method is regarded as the recommended method for supervised classification of polarimetric SAR data (6). The method can also be used for multi-frequency SAR data.

However, it requires a one-to-one correspondence on pixel-level between the single-look complex (SLC) data of all the used channels and it does not allow combining the covariance data with other types of features such as textural features or backscattered intensity. Alberga (7) showed that the approach based on the covariance matrix does provide important information about the scatterers on the ground, but that extra information (e.g. backscatter amplitude or texture) can be needed in order to distinguish complex classes.

This led us to the idea to develop an approach that allows taking into account a set of input features with diverse statistical properties, representing for instance radiometric, polarimetric and interferometric information. The developed approach combines feature selection with the combination of the features into a classification function.

The authors already developed (8) an approach based on logistic regression (LR), which considers each class separately and tries to distinguish it from all others by combining the input features into a non-linear function, the logistic function. The method allows us to add features easily. For each class, the logistic regression results in a "detection image", with a well-defined statistical meaning: the value at each pixel in the detection image represents the conditional probability that the pixel belongs to that class, given all input features. Moreover, the logistic regression implicitly performs a feature selection. The authors chose to use logistic regression because the statistical distribution of the used feature set is very diverse and the requirements for using LR are much less strict than for other methods such as linear discriminant analysis or classical regression. Other authors have dealt with this problem by developing classification methods based on fuzzy logic (9) or neural networks (10,11).

In this paper a large feature set is created, consisting of the results of various polarimetric decomposition methods, interferometric and polarimetric coherences, speckle reduced and original SAR data, etc. The main aim of the paper is to investigate the usefulness of each of these features for the detection of the different classes of interest. The paper is only concerned by the influence of the different features on the detection results for each class. For a discussion on the obtained classification results or on the methods to combine the detection results into a classification, the authors refer to earlier publications and in particular to (8). The developed classification method was compared to a method based on neural networks (11) and results were found to be similar. A detailed comparison is currently being performed and results will be submitted for publication.

THE DATASET

SAR data

The method was applied to a project on humanitarian demining (the *SMART* project) for which SAR data at 4 different frequencies were acquired by the E-SAR system of the German Aerospace Agency (DLR). P-band and L-band are full-polarimetric, dual-pass interferometric. For C-

and X-band only VV-polarisation was acquired. All data were delivered as Single-Look Complex (SLC) data as well as geocoded amplitude data. The pixel spacing in the SLC data of different bands is not the same. Therefore, the DLR also provided geocoding matrices that enable one to extract polarimetric and interferometric information using the SLC data and geocode the results afterwards. Table 1 presents principal characteristics of the SAR data.

The test area is an agricultural area in the South of Croatia and covers approximately 2 km by 4 km.

Table 1: Overview of the principal characteristics of the SAR data set

| Band | Wavelength (cm) | Polarization | Size in pixels (width x height) | Pixel Spacing (range x azimuth) |
|------|-----------------|--------------|---------------------------------|---------------------------------|
| P | 70 | HH, HV, VV | 1410 x 5790 | 1.50 m x 0.70 m |
| L | 23 | HH, HV, VV | 1452 x 9598 | 1.50 m x 0.43 m |
| C | 5.6 | VV | 1456 x 11350 | 1.50 m x 0.36 m |
| X | 3 | VV | 1455 x 11753 | 1.50 m x 0.35 m |

Ground Truth

A field survey mission was organized to acquire ground truth, i.e. the relevant classes of land-cover in the scene were determined and for each of them, examples were given. The ground truth objects were then divided into a learning set and a validation set. Both sets contain around 200 objects (regions) from the test-site. The learning set is used for the optimization of the parameters of the supervised classification. Table 2 shows the twelve classes used for the learning set for this test-site.

The agricultural fields were subdivided into C8: "Fields without vegetation (FieldsNV)" and the three types of crops that were visible at the time of image acquisition (barley, wheat and corn). The class C1: "abandoned land" refers to formerly cultivated land that has been abandoned. The class C6 can consist of single farms and was indicated as a region encircling the buildings. This means it can contain buildings, parking lots, roads and paths between the buildings, open spaces and trees. Agricultural fields in the region are often enclosed by hedges of large shrubs. This is class C11. The shadow class (C12) represents the radar shadows.

Table 2: Classes of interest defined for the project

| | | | | | | | |
|---|-----------|---|-------------|---|----------|----|---------|
| 1 | Abandoned | 4 | Wheat | 7 | Roads | 10 | Water |
| 2 | Pastures | 5 | Corn | 8 | FieldsNV | 11 | Hedges |
| 3 | Barley | 6 | Residential | 9 | Forests | 12 | Shadows |

THE DERIVED FEATURE SET

From the available SAR data, 80 features were derived. All features, except the line detector results, were determined on the SLC slant-range data and results geocoded. For features determined using a sliding window, a 5x5 window was used.

Radiometric Information

The considered radiometric information consists of:

- original amplitude data for each channel (8 features),
- speckle-reduced log-intensity data of each frequency and each polarisation (8 features). The speckle reduction method (12) combines a context-based, locally adaptive, wavelet

shrinkage and Markov Random Fields to limit blurring of edges, by incorporating prior knowledge about possible edge configurations.

Figures 1 and 2 show respectively the original SAR data of part of the scene and the same regions after applying the speckle reduction.

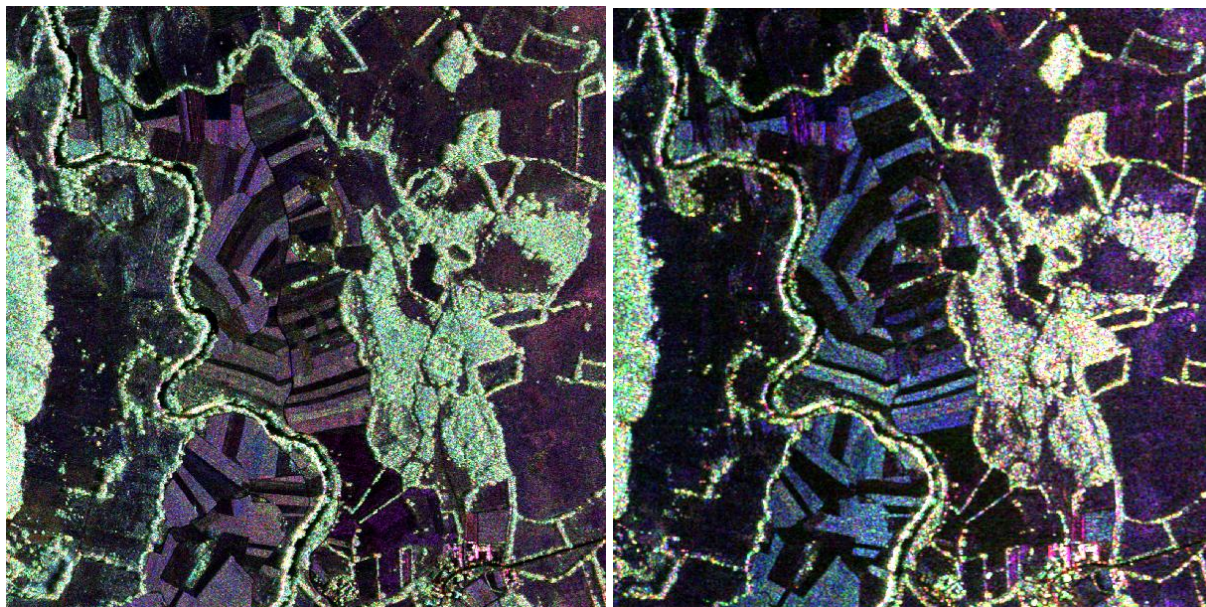


Figure 1: Original SAR images: left:L-band, right: P-band (R:HH, G:HV, B:VV)

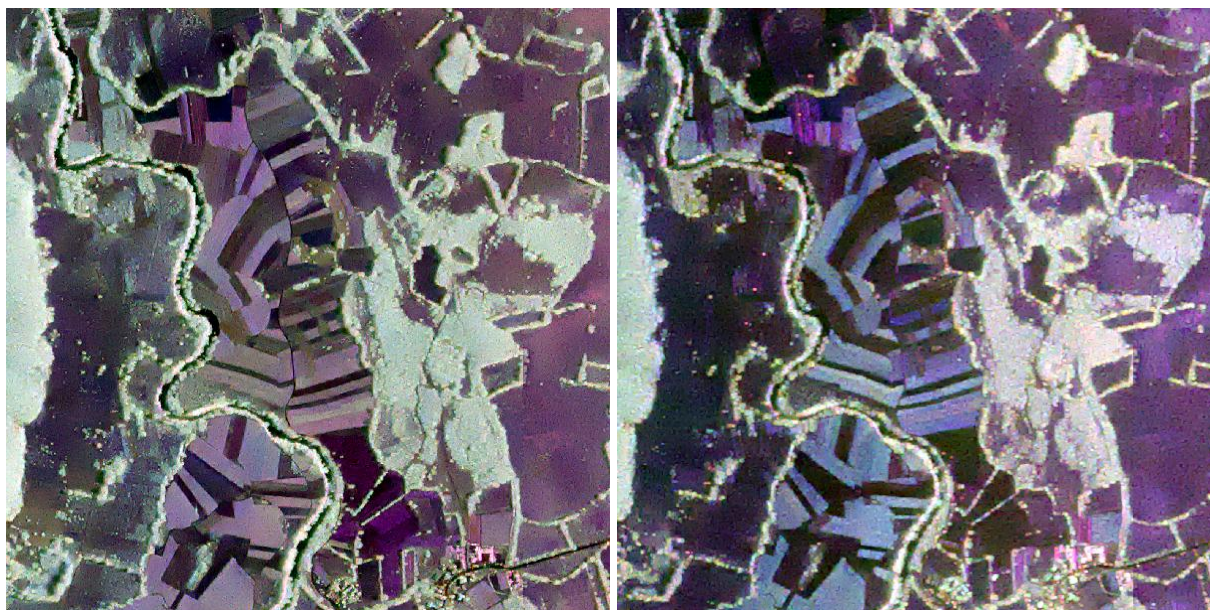


Figure 2: Speckle reduced SAR images. Left: L-band, right: P-band (R:HH, G:HV, B:VV)

Polarimetric Information

Different polarimetric decomposition methods were applied to the P- and L-band data. Decomposition methods combine the polarimetric information in a way that allows inferring information about the type of scattering produced by the elements on the ground on the radar waves. The most well known method is the Cloude & Pottier (2) decomposition. Several parameters were derived from their method: entropy H , scattering angle α , combinations of the entropy H and anisotropy A : HA , $H(1-A)$, $(1-H)A$ and $(1-H)(1-A)$ and the value of the largest eigenvalue of the polarimetric coherency matrix, λ_1 (14 features).

The other decomposition methods convert the polarimetric information into an abundance of three types of scattering. For applying these decomposition methods, the freely available software POLSARPRO was used. In this article the decomposition methods of Barnes and Holm (13), Huynen (14), Freeman (15) and Krogager (16) are considered. This leads to 24 features. The results of some of the polarimetric decomposition methods are shown in Figure 3.

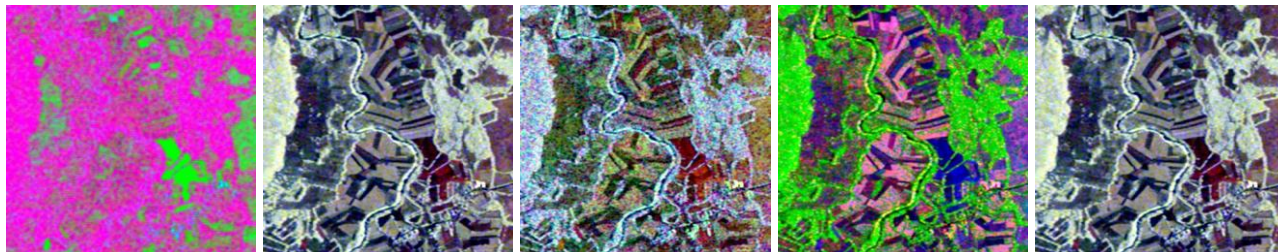


Figure 3: Results of the applied polarimetric decompositions. Left to right: Cloude, Huynen, Holm-Barnes, Freeman and Krogager.

Interferometric and polarimetric coherence information

Besides the parameters of the decomposition methods, the authors also considered the polarimetric coherence (i.e. the correlation between the different polarisations).

Analogously, from the pairs of dual-pass interferometric images, the interferometric coherences are calculated as well as the combined polarimetric/interferometric (PolIn) coherences. The total set of coherences consists of 24 features. Figure 4 shows the various coherence images obtained from the L-band SAR data.



Figure 4: L-band Coherence images: Polarimetric, Interferometric and PolIn coherence

Spatial Information

Some basic spatial information is included in the feature list. It consists of the results of a bright and a dark line detector (17). The line detector uses a multi-variate statistical test for detecting line structures and is applied on the 8 speckle reduced, geocoded, log-intensity images. These input channels are treated by the detector as a single vector input and a single result is obtained for the dark lines and another one for the bright lines (2 features). Figure 5 shows the results of the dark and bright line detector superimposed on the L-band VV component image.

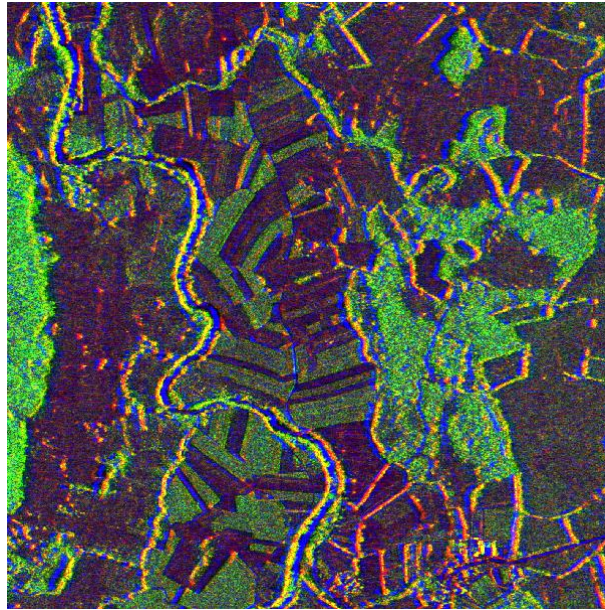


Figure 5: Results of the line detector (R: bright lines, G: L-VV image component, B: dark lines)

DETECTION AND CLASSIFICATION USING LOGISTIC REGRESSION

Logistic regression (LR) (18) is developed for dichotomous problems where a target class has to be distinguished from the background. The method combines the input parameters into a non-linear function, the logistic function:

$$p_{x,y}(\text{target} | \vec{C}) = \frac{\exp\left[\beta_0 + \sum_i F_i(x,y)\beta_i\right]}{1 + \exp\left[\beta_0 + \sum_i F_i(x,y)\beta_i\right]}$$

$p_{x,y}(\text{target} | \vec{F})$ is the conditional probability that a pixel (x,y) belongs to the considered class (target class) given the vector of input features \vec{F} at the given pixel. $F_i(x,y)$ is the value of pixel (x,y) in the i^{th} feature.

The logistic regression (i.e. the search for the weights β_i) is carried out using Wald's forward stepwise method using the commercial statistics software SPSS. In the Wald method, at each step, the most discriminating feature is added and the significance of adding it to the model is verified. This means that only the features that contribute significantly to the discrimination between the foreground and the background class are added to the model. The LR thus implicitly performs a feature selection.

Applying the obtained logistic function for a given target class to the complete image set, a new image - a 'detection image' - is obtained, in which the pixel value is proportional to the conditional probability that the pixel belongs to the target class, given the set of used features.

The detection images for the different classes are combined into a classification image by attributing to each pixel of the classification image the class that corresponds to the highest value of the detection image.

RESULTS AND DISCUSSION

The logistic regression was applied to find the best combination of several subsets of features. In order to compare the adequateness of each combination of features, each time the overall detection accuracy was determined for the different classes.

The subsets that were considered are:

- the full feature set
- all features leaving out the speckle reduced, the original amplitude and the interferometric data, respectively
- only the features derived from the L-band and P-band data, respectively
- only features derived from the Cloude & Pottier (CP) decomposition as polarimetric data
- for each of the other decomposition methods results were derived when the method is omitted from the feature set and when it is combined with the CP method

Table 3 presents the detection accuracy obtained by the logistic regression on the learning set. Results are shown for the different classes, for each of the defined subsets of features. In general, not using the speckle-reduced data degrades the detection performance. While the speckle reduction adds important information for the classifier, the original amplitude data are not useful.

The interferometric information only affects the results for the classes residential and wheat. Having only P- or L-band data degrades the results for almost all classes. For abandoned land, wheat, corn and residential areas, the P-band information is most important. For pastures, barley, roads, fields without vegetation, forests and hedges, the L-band information is most important.

It is very hard to derive a conclusion about the influence of the different polarimetric decomposition methods. From this table, all methods seem equivalent for most of the classes.

Tables 4-6 present an overview of the features that are selected by the logistic regression when the full set of features is given as input. The tables give results for each separate feature and for each class. The three tables represent three subsets of features, i.e. radiometric and spatial information, coherence information and polarimetric information. The bottom row of each table, labelled “# Selec.”, counts the number of classes for which each feature is selected. The columns labelled “# features” count the number of features that were selected by the logistic regression for distinguishing each class from the others in each of the subsets of features. The second column of Table 4 shows the total number of features that was selected for distinguishing each class from the others. The values in the table, corresponding to class/feature combinations, represent the order in which the different parameters were selected by the iterations of the step-wise logistic regression (e.g. for roads the first selected parameter is the HV polarised P-band original amplitude channel). As the logistic regression selects the features in decreasing significance for class detection, this number gives important information on the relevance of the features for detection.

Apparently most of the features were selected for at least one of the classes. The total number of selected features varies from 10 (for water and pastures) to 25 (for barley and wheat). Although one would expect the original amplitude data to be redundant with the speckle-reduced data, for most of the classes, combinations of both were selected. Exceptions are pastures, water and forests where only one of the two types of radiometric information is used.

The line detector results were selected for each class except water. Spatial information thus seems to be important.

Although, from the analysis in Table 3, the interferometric coherence parameters do not seem to influence the overall detection accuracy, they are selected for the majority of classes. From the coherence parameters, the interferometric coherence parameters are the most selected; the polarimetric coherence is only very rarely selected.

Table 3: Detection results (overall detection accuracy in %) for the different classes and for the various defined sub-sets of features

| | Abandoned | Pastures | Barley | Wheat | Corn | Residential | Roads | FieldsNV | Forests | Water | Hedges | Shadows |
|-------------------|-----------|----------|--------|-------|------|-------------|-------|----------|---------|-------|--------|---------|
| | 1 | 2 | 3 | 4 | 5 | 6 | 7 | 8 | 9 | 10 | 11 | 12 |
| All | 86.6 | 84.1 | 98.2 | 95.2 | 86.1 | 91.7 | 94.2 | 91.6 | 99.8 | 99.1 | 93.8 | 98.1 |
| No Speckle Red | 85.7 | 84.5 | 95.4 | 93.9 | 84.3 | 89.2 | 91.2 | 90.7 | 99.5 | 99.2 | 88.7 | 96.8 |
| No Amplitude | 87.2 | 84.8 | 98.2 | 96.7 | 86.2 | 91.5 | 94.6 | 91.5 | 99.5 | 99.4 | 94.5 | 98.2 |
| No Interferometry | 87.2 | 84.3 | 99.2 | 94.9 | 86.1 | 90.0 | 94.8 | 91.3 | 99.7 | 99.3 | 93.7 | 98.4 |
| Only Lband | 80.6 | 83.6 | 97.8 | 85.5 | 77.5 | 80.1 | 90.5 | 90.8 | 99.5 | 99.0 | 90.8 | 94.2 |
| Only Pband | 84.1 | 79.9 | 88.5 | 90.6 | 79.2 | 88.3 | 82.4 | 84.1 | 95.9 | 98.3 | 89.5 | 89.7 |
| Only CP | 86.1 | 85.3 | 98.7 | 95.7 | 84.8 | 90.7 | 94.8 | 89.8 | 99.5 | 99.4 | 93.8 | 97.3 |
| No CP | 87.4 | 84.4 | 98.1 | 95.5 | 86.1 | 89.4 | 94.1 | 90.6 | 99.5 | 99.4 | 93.6 | 97.7 |
| No Barnes | 87.4 | 85.3 | 98.8 | 95.4 | 86.1 | 91.3 | 94.4 | 92.2 | 99.9 | 99.5 | 94.4 | 98.4 |
| No Freeman | 87.6 | 85.7 | 98.9 | 95.3 | 86.8 | 92.0 | 94.3 | 92.7 | 99.9 | 99.2 | 93.9 | 97.4 |
| No Holms | 87.6 | 85.9 | 99.2 | 96.3 | 87.7 | 92.0 | 94.9 | 91.6 | 99.4 | 99.3 | 94.5 | 98.7 |
| No Huynen | 87.6 | 86.2 | 98.8 | 95.4 | 87.4 | 91.8 | 94.9 | 91.6 | 99.4 | 99.2 | 94.5 | 98.6 |
| No Krogager | 87.8 | 85.3 | 98.5 | 96.7 | 87.4 | 91.6 | 94.2 | 92.3 | 99.4 | 99.3 | 94.5 | 98.1 |
| CP+Barnes | 87.7 | 84.9 | 97.4 | 95.8 | 87.3 | 91.5 | 94.2 | 90.7 | 99.6 | 99.4 | 93.9 | 97.0 |
| CP+Freeman | 86.6 | 84.3 | 98.8 | 95.6 | 86.4 | 90.8 | 95.0 | 90.2 | 99.4 | 99.5 | 94.7 | 97.2 |
| CP+Holms | 86.7 | 85.0 | 98.7 | 95.6 | 86.3 | 90.8 | 94.7 | 91.5 | 99.5 | 99.4 | 94.4 | 97.5 |
| CP+Huynen | 86.4 | 85.3 | 98.3 | 95.8 | 86.4 | 92.0 | 94.6 | 91.6 | 99.5 | 99.4 | 94.3 | 97.4 |
| CP+Krogager | 86.5 | 85.0 | 98.7 | 95.8 | 86.3 | 90.7 | 95.4 | 92.1 | 99.5 | 99.6 | 94.3 | 97.8 |

Most of the polarimetric decomposition parameters were selected for at least one class. It seems that more of these parameters are used in L-band. L-band parameters were selected 54 times while the P-band parameters appear only 42 times. This can be explained by the fact that the backscattering mechanisms for the different classes are more discriminative at the shorter wavelength of the L-band (23 cm). The Holm decomposition is the least selected. The “spherical scattering” of Krogager was never selected. These results require a further analysis. In particular, it could be interesting to investigate the order in which the features are selected in the iterative LR process and how the feature selection changes when different sub-sets of features are given as input to the LR or to investigate the discrimination of the classes two-by-two.

CONCLUSION

A method for feature-based supervised classification, using logistic regression (LR), is presented. The method is applied on a set of multi-channel SAR data. Twelve classes were defined. The method is applied to discriminate each class from all others. A large feature set was determined. The main topic of the paper was to investigate the influence of these features on the overall detection accuracy and to use the feature selection property of the logistic regression to investigate the selection of parameters for the different classes. Most parameters seem relevant for at least one class. For the different polarimetric decomposition methods some seem much more effective than others. The interferometric coherence is more important than the polarimetric or the combined polarimetric/interferometric coherence. It could be useful to expand the feature set with new PolInSAR features such as proposed in 19 and 20. It is important to add spatial information to the feature set. This was done here by means of the results of line detectors. Other types of spatial

operators (e.g. texture parameters) should be examined. The obtained results need to be analysed further. In particular, it could be interesting to investigate how the feature selection changes when different sub-sets are given as input to the LR or to investigate the discrimination of the classes two-by-two.

The presented analysis is based on only one dataset. Results are likely to depend on the classes present in the scene, the environmental conditions (e.g. moisture) and topography and therefore a generalisation is not straightforward. So, it would be interesting to apply a similar analysis on several datasets. However, it is very difficult to obtain a comprehensive SAR dataset together with detailed ground truth. A joined effort of the SAR community for establishing a test database would be very welcome.

Table 4: Overview of selected radiometric and spatial parameters.

| | Tot. # Features | # Features | Speckle Reduction | | | | | | | | Original Amplitude | | | | | | | | LineDet | |
|--------------------|-----------------|------------|-------------------|----|----|----|----|----|----|----|--------------------|----|----|----|----|----|----|--------|---------|--|
| | | | HH | HV | VV | HH | HV | VV | VV | VV | HH | HV | VV | HH | HV | VV | VV | Bright | Dark | |
| | | | L | | | P | | | C | X | L | | | P | | | X | All | | |
| Abandoned Pastures | 20 | 9 | 11 | | | | 10 | 13 | 14 | 15 | 12 | | | 20 | 1 | | | 3 | | |
| Barley | 10 | 3 | | 7 | | | | | 6 | | | | | | | | | 3 | | |
| Wheat | 25 | 9 | 18 | | 9 | | | 15 | 10 | 14 | 6 | | 3 | | | 7 | 16 | | | |
| Corn | 25 | 10 | | | 23 | 7 | 17 | | 24 | | | | 25 | | 22 | 9 | 4 | 6 | 1 | |
| Resi | 17 | 8 | | 10 | 17 | 7 | | 14 | | | | 13 | 11 | | | | 9 | 12 | | |
| Roads | 23 | 7 | | 18 | 1 | 2 | | | | 6 | | 23 | | | | 17 | | 10 | | |
| FieldsNV | 17 | 8 | | 2 | 6 | 1 | | | 16 | 4 | | | | 14 | 7 | | | 5 | | |
| Forests | 15 | 5 | 3 | | | | 8 | | | | 12 | | | | 11 | | | 10 | | |
| Water | 11 | 3 | | | | | | | | | | 1 | 7 | | | | | 5 | | |
| Hedges | 10 | 5 | | | | | | | | | 6 | | 9 | 6 | | 3 | 7 | | | |
| Shadows | 13 | 4 | | 3 | | | | 2 | | | | | | | | 13 | | 1 | | |
| # Selec. | 16 | 5 | 11 | | | | | | | 12 | 13 | | | 14 | | | | 3 | | |
| # Selec. | | | 4 | 5 | 5 | 4 | 3 | 4 | 5 | 5 | 5 | 3 | 5 | 4 | 4 | 5 | 2 | 6 | 7 | |

Table 5: Overview of selected coherence parameters.

| | # Features | Coherence Measurements | | | | | | | | | | | | | | | | | |
|--------------------|------------|------------------------|----|----|----|----|----|---------|-------|-------|-------|-------|-------|--------------|-------|-------|-------|-------|-------|
| | | Interferometric | | | | | | Pol/Int | | | | | | Polarimetric | | | | | |
| | | HH | HV | VV | HH | HV | VV | HH/HV | HH/VV | VV/HV | VV/VV | HH/HV | HH/VV | VV/HV | VV/VV | HH/HV | HH/VV | VV/HV | VV/VV |
| | | L | | | P | | | L | | | P | | | L | | P | | | |
| Abandoned Pastures | 3 | 2 | 6 | | | 19 | | | | | | | | | | | | | |
| Barley | 3 | | | 2 | | 9 | 4 | | | | | | | | | | | | |
| Wheat | 3 | 17 | | | | | | 1 | 24 | | | | | | | | | | |
| Corn | 4 | 10 | | | 8 | 5 | | | | | | | 11 | | | | | | |
| Resi | 3 | 5 | | 8 | | | | | | 16 | | | | | | | | | |
| Roads | 4 | | 7 | 4 | | 16 | | | | | | | | | | | | 22 | |
| FieldsNV | 4 | | | | 11 | 8 | | | | 16 | | | | 10 | | | | | |
| Forests | 1 | | | | | | | 9 | | | | | | | | | | | |
| Water | 3 | 4 | | 2 | | 8 | | | | | | | | | | | | | |
| Hedges | 0 | | | | | | | | | | | | | | | | | | |
| Shadows | 2 | | | 5 | | 12 | | | | | | | | | | | | | |
| # Selec. | 0 | | | | | | | | | | | | | | | | | | |
| # Selec. | | 5 | 2 | 5 | 2 | 4 | 4 | 0 | 2 | 1 | 2 | 0 | 1 | 0 | 1 | 0 | 0 | 1 | 0 |

Table 6: Overview of selected polarimetric decomposition parameters.

| | # Features | Cloude | | | | | | | | | | | Barnes | | | | | | | | | | | | |
|--------------------|------------|-------------|-----|----------|-----|--------|--------|------------|-------------|-----|----------|-----|--------|--------|------------|-----|-----|-----|-----|----------|-----|----|----|----|----|
| | | λ_1 | H | α | HA | H(1-A) | (1-H)A | (1-H)(1-A) | λ_1 | H | α | HA | H(1-A) | (1-H)A | (1-H)(1-A) | T11 | T22 | T33 | T11 | T22 | T33 | | | | |
| | | L | | | | | | | P | | | | L | | | P | | | | | | | | | |
| Abandoned Pastures | 8 | | | | | 16 | | | | | | | | | | | | | 8 | | | | | | |
| Barley | 4 | | | 5 | 10 | | | | | | | | | | | | | | | | | | | | |
| Wheat | 13 | | | 8 | | | 11 | 4 | | 2 | | | | | | | 5 | | 21 | 19 | | | | | |
| Corn | 11 | 2 | | 20 | | | | 21 | | | | | | | | | | | | | | | | | |
| Resi | 6 | | | | | | | 7 | | | | | | | | | 2 | | | | 4 | | | | |
| Roads | 12 | | | | | 5 | | 11 | 15 | | | | | 13 | 14 | 19 | 8 | | | | 3 | | | | |
| FieldsNV | 5 | 13 | | | 9 | | | 15 | | | | | | | | | 3 | | | | | | | | |
| Forests | 9 | | 2 | | | | | 1 | | | | | | | | | | 5 | 4 | | | | | | |
| Water | 5 | | | | 10 | | 6 | | | | | | | | | | | | | | | | | | |
| Hedges | 5 | | 1 | | | | 4 | | | | 8 | | | | | | | | 10 | | | | | | |
| Shadows | 7 | | | 7 | | | 11 | 10 | | | 9 | | | | | | 6 | | | | | | | | |
| # Selec. | 11 | | 16 | | | | | 2 | 9 | | 4 | | | | | | 15 | | | | | | | | |
| | | 2 | 3 | 4 | 3 | 2 | 4 | 5 | 4 | 1 | 2 | 1 | 1 | 1 | 1 | 1 | 3 | 3 | 4 | 2 | 2 | | | | |
| | # Features | Freeman | | | | | | Holm | | | | | | Huynen | | | | | | Krogager | | | | | |
| | | Dbl | Odd | Vol | Dbl | Odd | Vol | T11 | T22 | T33 | T11 | T22 | T33 | T11 | T22 | T33 | T11 | T22 | T33 | Kd | Kh | Ks | Kd | Kh | Ks |
| | | L | | | P | | | L | | | P | | | L | | | P | | | L | | | P | | |
| Abandoned Pastures | 18 | 4 | 9 | 17 | | 5 | | | | | | | | | | | | | | | | | 7 | | |
| Barley | | | | 8 | | | | | | | | | | | | | | | | 1 | | | | | |
| Wheat | 1 | | | 24 | | | | 22 | | 25 | | 20 | | | 26 | | | | | | | | | 3 | |
| Corn | | | | 15 | 14 | 12 | | 13 | | 18 | | | | | 19 | 16 | | | | | | | | 15 | |
| Resi | | | 3 | | 1 | | | | | | | | | | | | | | | | | | | | |
| Roads | | | 9 | | | | 20 | | | | | | | | | 12 | | | | | | | | 21 | |
| FieldsNV | | | | | | | | | | | | | | | | | | | | | | | | | |
| Forests | 14 | | | | | 7 | | | | | | | | 13 | | | | | | 6 | 15 | | | | |
| Water | | | | | | | | 9 | | | | | | | 11 | | | | | 3 | | | | | |
| Hedges | | | | | 4 | | | | | | | | | | | | | | | | | | | 2 | |
| Shadows | | | | | | | | | | | | | | 8 | | | | | | | | | | | |
| # Selec. | 7 | | 6 | | | 1 | | | | | | | | 5 | | | | | | 8 | | | | 10 | |
| | | 4 | 1 | 4 | 4 | 3 | 4 | 1 | 3 | 0 | 0 | 2 | 0 | 4 | 1 | 0 | 0 | 3 | 1 | 4 | 2 | 0 | 5 | 1 | 0 |

ACKNOWLEDGEMENTS

The presented research is the result of a collaboration between several projects: a Belgian Defense project (F00/07) on *Semi-automatic Interpretation of SAR Images; Advanced SAR Technologies (ASARTECH)*, funded by the Belgian Science Policy (project no. SR/00/04) and *Space and Airborne Mined Area Reduction Tools (SMART)*, funded by the European Commission (project no. IST-2000-25044). M. Keller of the German Aerospace Center DLR provided the interferometric coherences. A. Pizurica of Ghent University provided the speckle reduction routines. All images were provided by DLR in the frame of the SMART project.

REFERENCES

1 Cloude S R & E Pottier, 1996. A review of target decomposition theorems in radar polarimetry. *IEEE Transactions on Geoscience and Remote Sensing*, 34: 498-518

- 2 Cloude S R & E Pottier, 1997. An entropy based classification scheme for land applications of polarimetric SAR. IEEE Transactions on Geoscience and Remote Sensing, 35: 68-78
- 3 Lee J, M Grunes, T Ainsworth, L Du, D Schuler & S Cloude, 1999. Unsupervised classification using polarimetric decomposition and the complex Wishart classifier. IEEE Transactions on Geoscience and Remote Sensing, 37, 2249-2257
- 4 Hellmann M, 2000, Classification of fully polarimetric SAR-data for cartographic applications. PhD Thesis, Fakultät Elektrotechnik der Technischen Universität Dresden, Dresden. Deutsches Zentrum für Luft- und Raumfahrt (DLR), Research Report no. 2000-19, 170 pp.
- 5 Lee J, M Grunes & G de Grandi, 1999. Polarimetric SAR speckle filtering and its implication for classification, IEEE Transactions on Geoscience and Remote Sensing, 37: 2363-2373
- 6 Rodrigues A, D G Corr, E Pottier, F Ferro-Famil & D Hoekman, 2003. Land cover classification using polarimetric SAR data. POLinSAR 2003, (ESA-ESRIN, Frascati) 10 pp.
- 7 Alberga V., 2003. Comparison of polarimetric methods in image classification and SAR interferometry applications. PhD thesis, Fakultät für Elektrotechnik und Informationstechnik der Technischen Universität at Chemnitz, Dresden. Deutsches Zentrum für Luft- und Raumfahrt (DLR), Research Report No. 2004-05, 195 pp.
- 8 Borghys D, Y Yvinec, C Perneel, A Pizurica & W Philips, 2006. Supervised feature-based classification of multi-channel SAR images, Pattern Recognition Letters, Special issue on pattern recognition for remote sensing, 27(4): 252-258
- 9 Corr DG, A Walker, U Benz, I Lingenfelder & A Rodrigues, 2003. Classification of urban SAR imagery using object oriented techniques. Proceedings of IGARSS'03 (Toulouse, France, 21-25 July) 188-190
- 10 Chen K S, W P Huang, D H Tsay & F Amar, 1996. Classification of multi-frequency SAR imagery using a dynamic learning neural network. IEEE Transactions on Geoscience and Remote Sensing, 34(3): 814-820
- 11 Alberga V, G Satalino & D K Staykova, 2006. Polarimetric SAR observables for land cover classification: analyses and comparisons. In: SAR Image Analysis, Modeling, and Techniques VIII, edited by C Notarnicola, S R J Axelsson & F Posa. Proceedings of SPIE. 6363: 636305
- 12 Pizurica A, W Philips, I Lemahieu & M Acheroy, 2001. Despeckling SAR images using wavelets and a new class of adaptive shrinkage estimators, In: Proceedings IEEE 2001 Conference on Image Processing, 2: 233-236
- 13 Holm W & R M Barnes 1988. On radar polarization mixed target state decomposition techniques In: IEEE Proceedings 1988 National Radar Conference (Ann Arbor, MI, USA) pp 249-254
- 14 Huynen J R, 1970. Phenomenological Theory of Radar Targets. PhD thesis, University of Technology, Delft, The Netherlands
- 15 Freeman A & S L Durden, 1997. A three-component scattering model for polarimetric SAR data. IEEE Transactions on Geoscience and Remote Sensing, 36(1), 68-78
- 16 Krogager E, 1993. Aspects of polarimetric radar imaging. PhD Thesis, Technical University of Denmark, Electromagnetics Institute
- 17 Borghys D, A Pizurica, C Perneel & W Philips, 2003. Combining multi-variate statistics and speckle reduction for line detection in multi-channel SAR images. In: Proceedings of SAR Image Analysis, Modeling, and Techniques VI, edited by F Posa. Proceedings of SPIE, 5236: 93-104

- 18 Hosmer D & S Lemeshow, 2000. Applied Logistic Regression, 2nd Edition (John Wiley & Sons Inc, New York) 375 pp.
- 19 Neumann M, A Reigber & L Ferro-Famil, 2005. Data classification based on PolInSAR coherence shapes. Proceedings IGARSS'05 (Seoul, Korea) 4852–4855
- 20 Lee J S, M R Grunes, T Ainsworth, I Hajnsek, T Mette & K P Papathanassiou, 2005. [Forest classification based on L-band polarimetric and interferometric SAR data. POLInSAR 2005](#) (ESA-ESRIN, Frascati) 7 pp.